

Journal of Organometallic Chemistry, 405 (1991) 121–132
Elsevier Sequoia S.A., Lausanne
JOM 21425

Pentadienyl-metal-phosphine chemistry

XXI *. Synthesis and characterization of electron-rich (pentadienyl)iron[1,2-bis(diethylphosphino)ethane] complexes

John R. Blecke * and Robert J. Wittenbrink

Department of Chemistry, Washington University, St. Louis, MO 63130 (USA)

(Received August 6th, 1990)

Abstract

Treatment of $(Cl)_2Fe(depe)_2$ ($depe = Et_2PCH_2CH_2PEt_2$) with two equivalents of potassium pentadienide produces $(\eta^3\text{-pentadienyl})_2Fe(depe)$ (**1**). Compound **1** crystallizes in the orthorhombic space group *Pbcn* (No. 60) with $a = 11.347(1)$, $b = 9.718(2)$, $c = 19.938(3)$ Å, $V = 2198.6(6)$ Å³, and $Z = 4$. In the solid state structure of **1**, both η^3 -pentadienyl ligands are *syn* and W-shaped; however, in solution the major “*syn, syn*” isomer exists in equilibrium with a minor “*syn, anti*” isomer.

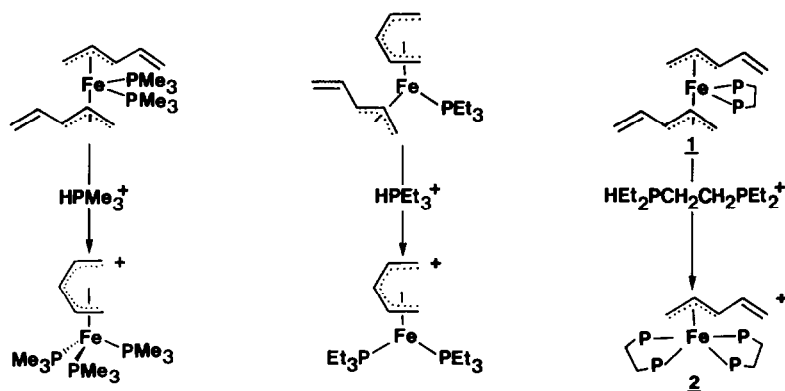
Treatment of compound **1** with one equivalent of protonated *depe* ($Hdepe^+ BF_4^-$) leads to loss of *trans*-1,3-pentadiene and production of $(\eta^3\text{-pentadienyl})Fe(depe)_2^+ BF_4^-$ (**2**). Compound **2** crystallizes in the triclinic space group *P1* (No. 1) with $a = 10.070(2)$, $b = 10.756(1)$, $c = 8.3622(1)$ Å, $\alpha = 112.04(2)$, $\beta = 94.93(1)$, $\gamma = 68.05(1)^\circ$, $V = 777.1(3)$ Å³, and $Z = 1$. In the solid state structure of **2**, the η^3 -pentadienyl ligand has a *syn* geometry and is W-shaped. In solution, the *syn*- η^3 -pentadienyl complex exists in equilibrium with its *anti*- η^3 -pentadienyl isomer.

Introduction

During the past several years, there has been increasing interest in the chemistry of transition metal complexes containing the acyclic pentadienyl ligand [2]. In part, this interest has been spurred by the pentadienyl ligand's demonstrated ability to adopt a variety of bonding modes (including η^5 , η^3 , and η^1 modes) and expectations that interconversions between these bonding modes will lead to interesting stoichiometric or even catalytic chemistry.

Recently, we have begun to investigate the synthesis, structure, and solution dynamics of (mono-pentadienyl)iron(phosphine) cationic complexes [1k,o,t]. One promising synthetic approach to this compound class involves protonation of neutral (bis-pentadienyl)iron(phosphine) complexes in the presence of additional

* For the previous papers in this series, see ref. 1.



Scheme 1

phosphine ligands. As examples of this approach, we have reported that treatment of $(\eta^3\text{-pentadienyl})_2\text{Fe}(\text{PMe}_3)_2$ [1b] with protonated trimethylphosphine (HPMe_3^+) leads to the production of $(\eta^3\text{-pentadienyl})\text{Fe}(\text{PMe}_3)_3^+$ [1k], while treatment of $(\eta^5\text{-pentadienyl})(\eta^3\text{-pentadienyl})\text{Fe}(\text{PEt}_3)$ [1o] with protonated triethylphosphine (HPEt_3^+) produces $16e^- (\eta^5\text{-pentadienyl})\text{Fe}(\text{PEt}_3)_2^+$ [1t]. We now report that this general synthetic method can be extended to complexes containing chelating diphosphine ligands. In particular, we have found that treatment of $(\eta^3\text{-pentadienyl})_2\text{Fe}(\text{depe})$ ($\text{depe} = \text{Et}_2\text{PCH}_2\text{CH}_2\text{PEt}_2$) with protonated depe (Hdepe^+) produces $(\eta^3\text{-pentadienyl})\text{Fe}(\text{depe})_2^+$. Taken together, these three protonation reactions (Scheme 1) dramatically demonstrate the key role of ligand steric and chelating effects in determining product composition.

Results and discussion

A. Synthesis and characterization of $(\eta^3\text{-pentadienyl})_2\text{Fe}(\text{Et}_2\text{PCH}_2\text{CH}_2\text{PEt}_2)$ (1)

Treatment of $\text{Fe}(\text{Cl})_2(\text{depe})_2$ [3] ($\text{depe} = \text{Et}_2\text{PCH}_2\text{CH}_2\text{PEt}_2$) with two equivalents of potassium pentadienide · tetrahydrofuran [4] leads to the clean production of red $(\eta^3\text{-pentadienyl})_2\text{Fe}(\text{depe})$ (1). The solid state structure of 1, derived from a single crystal X-ray diffraction study, is shown in Fig. 1. Positional parameters of the non-hydrogen atoms are listed in Table 1, while selected bond distances and angles are given in Table 2. The molecular geometry is pseudooctahedral; the six coordination sites around the iron atom are occupied by the two Cl atoms and two C3 atoms of the pentadienyl ligands and the two P atoms of the depe ligand. Deviations from true octahedral geometry result from the small bite angles of the $\eta^3\text{-pentadienyl}$ ligands ($68.4(3)^\circ$) and the depe ligand ($85.72(9)^\circ$). The central iron atom resides on a crystallographically imposed C_2 axis which bisects the P–Fe–P angle. The two pentadienyl ligands and the two ends of the depe ligand are symmetry-related by this 2-fold rotation axis.

The pentadienyl ligands are oriented so that the “mouths” of their allylic (iron-bound) moieties face the phosphine groups (i.e., the “mouth” made by Cl, C2, and C3 faces P1). Cl of one pentadienyl ligand is *trans* to Cl of the other pentadienyl ligand, while the two C3 atoms are *trans* to phosphorus atoms. The $\eta^3\text{-pentadienyl}$ ligands are *syn* and W-shaped with torsional angles of -176.7° and

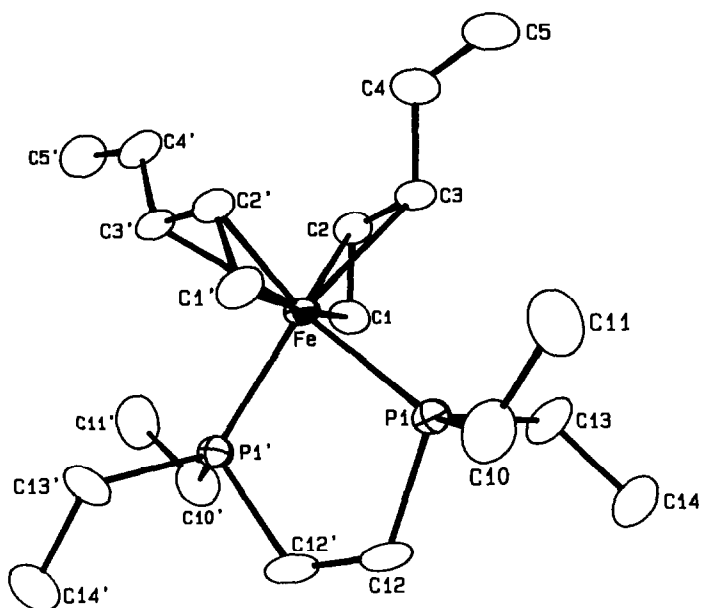


Fig. 1. ORTEP drawing of $(\eta^3\text{-pentadienyl})_2\text{Fe}(\text{Et}_2\text{PCH}_2\text{CH}_2\text{PEt}_2)$ (**1**).

-167.5° for C1–C2–C3–C4 and C2–C3–C4–C5, respectively. As with other *syn*- η^3 -pentadienyl ligands, C1, C2, C3 and C4 are essentially coplanar while C5 resides 0.21 Å out of the plane away from the iron atom [5]. The dihedral angle between plane C1–C2–C3 and plane C3–C4–C5 is 14.5° . Overall, the structure of **1** very closely resembles that of $(\eta^3\text{-pentadienyl})_2\text{Fe}(\text{PMe}_3)_2$, which we reported earlier [1b].

In solution, **1** exists as an equilibrium mixture of two isomers. The major solution-phase species (70%) is the “*syn,syn*” isomer, whose crystal structure has been described above. Its two pentadienyl ligands and its two depe phosphorus

Table 1

Positional parameters and their estimated standard deviations for non-hydrogen atoms in $(\eta^3\text{-pentadienyl})_2\text{Fe}(\text{Et}_2\text{PCH}_2\text{CH}_2\text{PEt}_2)$ (**1**)

Atom	x	y	z
Fe	0.500	0.1524(1)	0.750
P1	0.5050(2)	0.3202(2)	0.67416(9)
C1	0.6864(6)	0.1424(7)	0.7585(4)
C2	0.6383(6)	0.0226(7)	0.7352(4)
C3	0.5773(6)	0.0109(7)	0.6744(4)
C4	0.5221(8)	-0.1174(8)	0.6532(5)
C5	0.481(1)	-0.1456(9)	0.5931(5)
C10	0.3782(8)	0.354(1)	0.6188(5)
C11	0.359(1)	0.247(1)	0.5692(4)
C12	0.511(1)	0.4890(7)	0.7196(4)
C13	0.6297(7)	0.3438(8)	0.6179(5)
C14	0.6385(8)	0.4651(9)	0.5726(4)

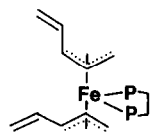
Table 2

Selected bond distances (Å) and bond angles (deg) with estimated standard deviations for (η^3 -pentadienyl) $_2$ Fe(Et $_2$ PCH $_2$ CH $_2$ PEt $_2$) (1)

Fe–P1	2.225(2)	P1–C10	1.843(9)
Fe–C1	2.123(6)	P1–C12	1.875(7)
Fe–C2	2.035(6)	P1–C13	1.821(7)
Fe–C3	2.221(6)	C10–C11	1.45(1)
C1–C2	1.367(9)	C13–C14	1.487(9)
C2–C3	1.400(9)	C12–C12'	1.24(2) ^a
C3–C4	1.458(9)		
C4–C5	1.32(1)		
P1–Fe–P1'	85.72(9)	C10–P1–C12	99.0(5)
P1–Fe–C1	93.6(2)	C10–P1–C13	102.4(4)
P1–Fe–C1'	90.3(2)	C12–P1–C13	99.3(5)
P1–Fe–C3	89.0(2)	P1–C10–C11	113.3(8)
P1–Fe–C3'	157.7(2)	P1–C12–C12'	117.9(4)
C1–Fe–C1'	174.8(3)	P1–C13–C14	121.7(6)
C1–Fe–C3	68.4(3)	C1–C2–C3	124.1(7)
C1–Fe–C3'	108.1(3)	C2–C3–C4	122.2(8)
C3–Fe–C3'	103.5(4)	C3–C4–C5	126.6(9)
Fe–P1–C10	121.3(3)		
Fe–P1–C12	108.3(2)		
Fe–P1–C13	122.1(3)		

^a The apparent shortness of this C–C single bond can be attributed to an unresolved two-fold disorder in the positions of C12/C12'.

atoms are equivalent by NMR. The minor solution phase isomer appears to be the “*syn,anti*” isomer, (*syn*- η^3 -pentadienyl)(*anti*- η^3 -pentadienyl)Fe(depe) (see below). In this species, the two pentadienyl ligands are inequivalent, as are the two depe phosphorus atoms.



'*syn,anti*' isomer

B. Synthesis and characterization of (η^3 -pentadienyl)Fe(Et $_2$ PCH $_2$ CH $_2$ PEt $_2$) $_2^+$ BF $_4^-$ (2)

Treatment of (η^3 -pentadienyl) $_2$ Fe(depe) (depe = Et $_2$ PCH $_2$ CH $_2$ PEt $_2$) (1) with one equivalent of protonated depe (Hdepe $^+$ BF $_4^-$) produces red (η^3 -pentadienyl)Fe(depe) $_2^+$ BF $_4^-$ in high yield [6*]. The chelating ability of the depe, together with its small cone angle (per phosphorus) [7], accounts for the stability of the “P $_4$ ” product in this system, as compared with the “P $_3$ ” and “P $_2$ ” products formed in the analogous PMe $_3$ and PEt $_3$ systems, respectively (Scheme 1).

This protonation reaction probably proceeds by initial H $^+$ attack at the iron center, followed by rapid migration of the “hydride” ligand to the terminal carbon of an η^3 -pentadienyl group. The resulting η^2 -pentadiene ligand is then displaced by an incoming depe molecule [8*].

* A reference number with an asterisk indicates a note in the list of references.

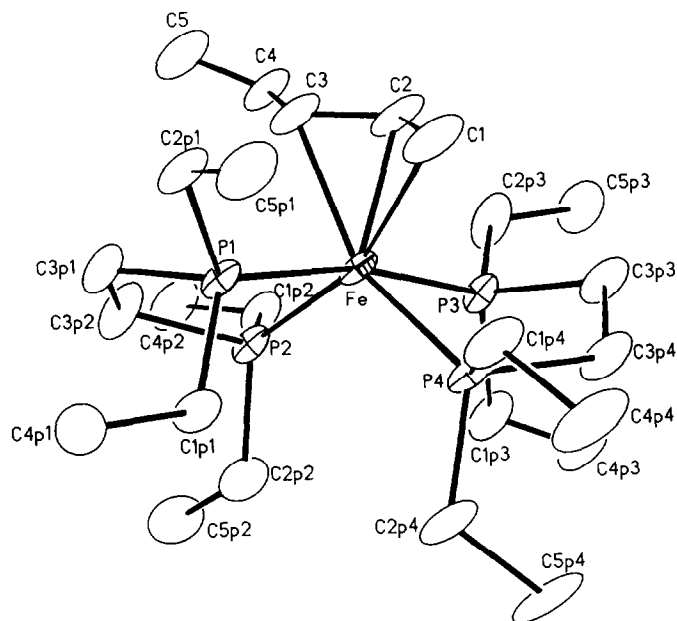


Fig. 2. ORTEP drawing of the cation in $(\eta^3\text{-pentadienyl})\text{Fe}(\text{Et}_2\text{PCH}_2\text{CH}_2\text{PEt}_2)_2^+ \text{BF}_4^-$ (**2**).

The solid state structure of $(\eta^3\text{-pentadienyl})\text{Fe}(\text{depe})_2^+ \text{BF}_4^-$ (**2**) has been determined by X-ray crystallography and is shown in Fig. 2. Positional parameters of the non-hydrogen atoms are listed in Table 3, while selected bond distances and angles are given in Table 4. The molecule assumes a pseudo-octahedral coordination geometry wherein the four phosphorus atoms and C1 and C3 of the pentadienyl ligand occupy the six coordination sites. Deviations from true octahedral geometry result from the small bite angles of the depe ligands ($82.77(6)^\circ$ and $79.46(6)^\circ$) and the $\eta^3\text{-pentadienyl}$ ligand ($67.3(3)^\circ$). The pentadienyl ligand is *syn* and W-shaped with torsional angles of $178.1(7)^\circ$ and $-155.6(9)^\circ$ for C1–C2–C3–C4 and C2–C3–C4–C5, respectively. Pentadienyl carbon atoms C1, C2, C3 and C4 are essentially coplanar, while C5 resides $0.45(1)$ Å out of the plane away from the iron atom. The dihedral angle made by planes C1–C2–C3 and C3–C4–C5 is 23.5° . The structure of **2** very closely resembles that of isoelectronic $(\text{syn-}\eta^3\text{-pentadienyl})\text{Mn}(\text{Me}_2\text{PCH}_2\text{-CH}_2\text{PMe}_2)_2$, which we reported earlier [1d].

In solution at -40°C , $(\text{syn-}\eta^3\text{-pentadienyl})\text{Fe}(\text{depe})_2^+ \text{BF}_4^-$ is in equilibrium with its *anti-}\eta^3\text{-pentadienyl}* isomer [9*]. The two isomers, which are present in almost equal concentrations, can be seen clearly in the $^{13}\text{C}\{^1\text{H}\}$ NMR spectrum; the *syn-}\eta^3\text{-pentadienyl}* and *anti-}\eta^3\text{-pentadienyl}* carbon atoms give rise to closely-spaced pairs of signals. In the $^{31}\text{P}\{^1\text{H}\}$ NMR spectrum at -40°C , each isomer gives rise to a complicated second-order ABCD pattern. The two overlapping ABCD patterns can be distinguished from one another by using ^{31}P – ^{31}P shift-correlated (COSY) 2D NMR spectroscopy and then simulated using the spin simulation program, LAME. Shown in Fig. 3 are the calculated and experimental (-40°C) $^{31}\text{P}\{^1\text{H}\}$ NMR spectra for the isomer mixture. Calculated ^{31}P NMR chemical shifts and coupling constants for each isomer are given in the Experimental Section.

Table 3

Positional parameters and their estimated standard deviations for non-hydrogen atoms in (η^3 -pentadienyl)Fe(Et₂PCH₂CH₂PEt₂)₂⁺BF₄⁻ (**2**)

Atom	x	y	z
<i>Cation</i>			
Fe	0.000	0.000	0.000
P1	-0.1937(2)	0.1456(2)	0.1886(2)
P2	-0.0517(2)	-0.1748(2)	0.0328(2)
P3	0.2143(2)	-0.1641(2)	-0.1432(2)
P4	0.1548(2)	0.0815(2)	0.1831(2)
C1	-0.0149(8)	0.1703(7)	-0.0895(9)
C2	-0.0354(7)	0.0491(7)	-0.2197(8)
C3	-0.1527(7)	0.0136(7)	-0.2107(8)
C4	-0.1757(7)	-0.1071(8)	-0.3458(9)
C5	-0.2995(9)	-0.122(1)	-0.382(1)
C1P1	-0.1705(8)	0.1865(7)	0.4215(9)
C2P1	-0.3213(8)	0.3217(7)	0.185(1)
C3P1	-0.3175(7)	0.0498(7)	0.145(1)
C4P1	-0.306(1)	0.263(1)	0.544(1)
C5P1	-0.2791(9)	0.4540(8)	0.273(1)
C1P2	-0.0129(7)	-0.3470(7)	-0.156(1)
C2P2	0.0214(8)	-0.2401(7)	0.2074(9)
C3P2	-0.2462(8)	-0.1077(8)	0.084(1)
C4P2	-0.1172(9)	-0.4273(9)	-0.192(1)
C5P2	-0.015(1)	-0.3615(7)	0.220(1)
C1P3	0.3250(7)	-0.2876(7)	-0.039(1)
C2P3	0.2320(9)	-0.283(1)	-0.372(1)
C3P3	0.3267(7)	-0.0584(7)	-0.1298(9)
C4P3	0.4868(8)	-0.3607(9)	-0.082(1)
C5P3	0.363(1)	-0.336(1)	-0.483(1)
C1P4	0.1040(8)	0.2795(7)	0.283(1)
C2P4	0.2107(8)	0.0268(8)	0.3723(9)
C3P4	0.3276(7)	0.0299(7)	0.0619(9)
C4P4	0.2175(9)	0.3327(8)	0.397(1)
C5P4	0.3682(8)	-0.0041(9)	0.423(1)
<i>Anion</i>			
B	0.3498(9)	0.3185(9)	0.883(1)
F1	0.4563(7)	0.1954(6)	0.8757(9)
F2	0.3761(7)	0.3697(5)	0.7707(8)
F3	0.2250(6)	0.2922(7)	0.842(1)
F4	0.3307(9)	0.4222(8)	1.0483(9)

In solution, at temperatures higher than -20°C , **2** begins to slowly decompose to paramagnetic products. As a result, NMR spectra of **2** taken at room temperature are invariably broad and shifted.

Experimental

General comments

All manipulations were carried out under inert atmosphere, using either drybox or Schlenk techniques. Diethyl ether, tetrahydrofuran, and toluene were dried with sodium/benzophenone and distilled before use. Pentane was dried over calcium

Table 4

Selected bond distances (Å) and bond angles (deg) with estimated standard deviations for $(\eta^3\text{-pentadienyl})\text{Fe}(\text{Et}_2\text{PCH}_2\text{CH}_2\text{PEt}_2)_2^+\text{BF}_4^-(2)$

Fe-P1	2.267(2)	P3-C1P3	1.835(9)	C1P2-C4P2	1.54(1)
Fe-P2	2.242(2)	P3-C2P3	1.836(9)	C2P2-C5P2	1.52(1)
Fe-P3	2.284(1)	P3-C3P3	1.851(9)	C1P3-C4P3	1.53(1)
Fe-P4	2.269(2)	P4-C1P4	1.849(7)	C2P3-C5P3	1.48(1)
Fe-C1	2.178(9)	P4-C2P4	1.862(9)	C3P3-C3P4	1.527(9)
Fe-C2	2.063(8)	P4-C3P4	1.877(8)	C1P4-C4P4	1.56(1)
Fe-C3	2.248(7)	C1-C2	1.42(1)	C2P4-C5P4	1.55(1)
P1-C1P1	1.842(8)	C2-C3	1.39(1)	B-F1	1.34(1)
P1-C2P1	1.859(7)	C3-C4	1.45(1)	B-F2	1.34(1)
P1-C3P1	1.829(9)	C4-C5	1.31(1)	B-F3	1.38(1)
P2-C1P2	1.857(6)	C1P1-C4P1	1.54(1)	B-F4	1.38(1)
P2-C2P2	1.834(8)	C2P1-C5P1	1.54(1)		
P2-C3P2	1.843(8)	C3P1-C3P2	1.47(1)		
P1-Fe-P2	82.77(6)	P4-Fe-C1	83.5(2)	Fe-P4-C1P4	116.6(3)
P1-Fe-P3	167.67(7)	P4-Fe-C3	150.8(2)	Fe-P4-C2P4	120.7(3)
P1-Fe-P4	93.95(6)	C1-Fe-C3	67.3(3)	Fe-P4-C3P4	110.4(2)
P1-Fe-C1	92.2(2)	Fe-P1-C1P1	118.8(2)	C1-C2-C3	121.7(6)
P1-Fe-C3	86.6(2)	Fe-P1-C2P1	124.0(3)	C2-C3-C4	121.7(6)
P2-Fe-P3	90.84(7)	Fe-P1-C3P1	106.7(2)	C3-C4-C5	126.0(6)
P2-Fe-P4	116.69(7)	Fe-P2-C1P2	117.6(3)	F1-B-F2	111.6(8)
P2-Fe-C1	159.4(2)	Fe-P2-C2P2	120.8(3)	F1-B-F3	108.9(8)
P2-Fe-C3	92.3(2)	Fe-P2-C3P2	108.4(3)	F1-B-F4	110.3(8)
P3-Fe-P4	79.46(6)	Fe-P3-C1P3	115.9(3)	F2-B-F3	108.1(8)
P3-Fe-C1	97.3(2)	Fe-P3-C2P3	123.4(3)	F2-B-F4	108.9(8)
P3-Fe-C3	104.3(2)	Fe-P3-C3P3	105.8(2)	F3-B-F4	109.0(8)

hydride and distilled. $\text{Hdepe}^+\text{BF}_4^-$ was prepared by treating 1,2-bis(diethylphosphino)ethane (Strem) with $\text{HBF}_4 \cdot \text{OEt}_2$ (Aldrich) in diethyl ether, followed by filtering the precipitated product. $\text{FeCl}_2(\text{Et}_2\text{PCH}_2\text{CH}_2\text{PEt}_2)_2$ was prepared by the method of Chatt [3]. Potassium pentadienide · tetrahydrofuran was prepared by the method of Yasuda and Nakamura [4].

NMR experiments were performed on a Varian XL-300 or Gemini 300 (^1H , 300 MHz; ^{13}C , 75 MHz; ^{31}P , 121 MHz) NMR spectrometer. ^1H and ^{13}C spectra were referenced to tetramethylsilane. ^{31}P spectra were referenced to external H_3PO_4 . The spin simulation of the $^{31}\text{P}\{^1\text{H}\}$ NMR spectrum of **2** (Fig. 3) was done on a SUN-3 Host Computer System using program LAME of the VXR-5000 software package. LAME calculates the theoretical spectra for spin 1/2 nuclei, given the chemical shifts and coupling constants. Parameters were adjusted by iteration to approach the experimental spectra. For the iterative runs, one parameter was held constant (e.g., chemical shift) while the other was adjusted (e.g., coupling constant). This process was repeated until a convergence of theoretical and experimental spectra was achieved.

Microanalyses were performed by Galbraith Laboratories, Inc., Knoxville, TN.

$(\eta^3\text{-Pentadienyl})_2\text{Fe}(\text{Et}_2\text{PCH}_2\text{CH}_2\text{PEt}_2)_2$ (**1**)

Potassium pentadienide · THF (0.71 g, 4.0×10^{-3} mol) in 75 ml of THF was added dropwise to a cold (-78°C) stirred solution of $\text{FeCl}_2(\text{Et}_2\text{PCH}_2\text{CH}_2\text{PEt}_2)_2$

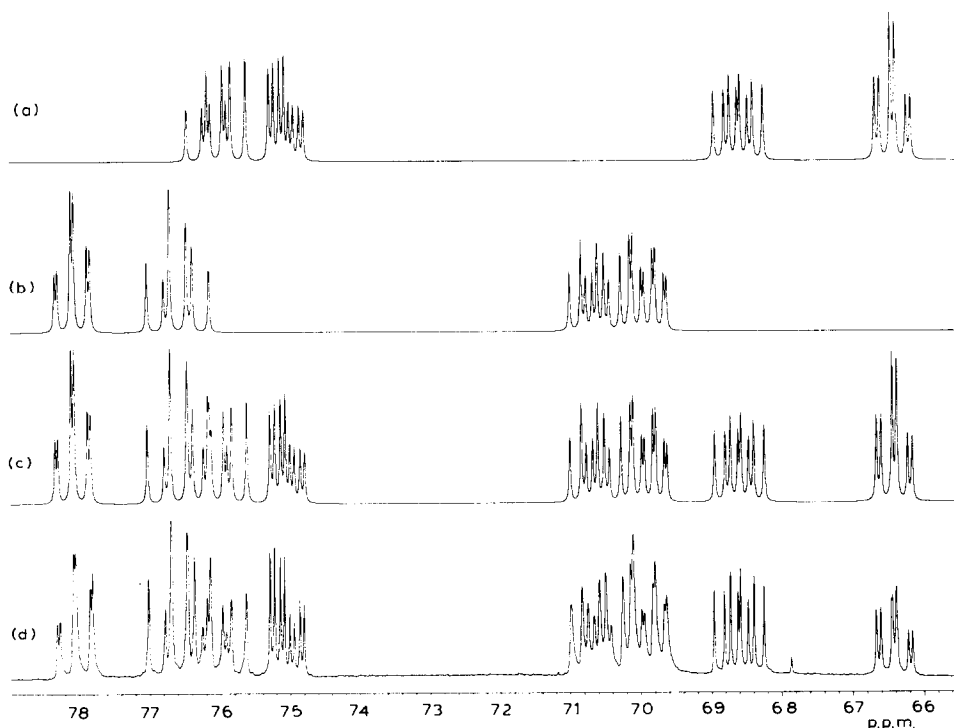


Fig. 3. (a) Simulated $^{31}\text{P}\{^1\text{H}\}$ NMR spectrum for Isomer 1 of $(\eta^3\text{-pentadienyl})\text{Fe}(\text{Et}_2\text{PCH}_2\text{CH}_2\text{PEt}_2)_2^+ \text{BF}_4^-$ (**2**). (b) Simulated $^{31}\text{P}\{^1\text{H}\}$ NMR spectrum for Isomer 2 of **2**. (c) Sum of simulated spectra in (a) and (b). (d) Experimental $^{31}\text{P}\{^1\text{H}\}$ NMR spectrum of **2** at -40°C .

(1.08 g, 2.0×10^{-3} mol) in 75 ml of THF. After the addition was complete the solution was allowed to warm slowly to room temperature and stirred for an additional 2 h. The solution was then filtered through Celite and the solvent was removed under vacuum, leaving a dark red solid which was extracted with pentane. The resultant pentane solution was then filtered through Celite, concentrated, and cooled to -30°C . The product crystallized as dark red plates. Second and third crops were obtained by concentrating the mother liquor and cooling to -30°C . Yield of crystalline product: 0.56 g (71%). Anal. Found: C, 60.90; H, 9.83. $\text{C}_{20}\text{H}_{38}\text{FeP}_2$ calcd.: C, 60.60; H, 9.68%.

Compound **1** crystallized as $(\text{syn-}\eta^3\text{-pentadienyl})_2\text{Fe}(\text{Et}_2\text{PCH}_2\text{CH}_2\text{PEt}_2)$. However, in solution at 20°C , this species existed in equilibrium with a minor isomer, believed to be $(\text{syn-}\eta^3\text{-pentadienyl})(\text{anti-}\eta^3\text{-pentadienyl})\text{Fe}(\text{Et}_2\text{PCH}_2\text{CH}_2\text{PEt}_2)$.

Major isomer, $(\text{syn-}\eta^3\text{-pentadienyl})_2\text{Fe}(\text{Et}_2\text{PCH}_2\text{CH}_2\text{PEt}_2)$ (70%). ^1H NMR (20°C , benzene- d_6): δ 6.41 (m, 2, H4), 5.22 (d, $J(\text{H-H}) = 12$ Hz, 2, H5_{syn}), 5.10 (d, $J(\text{H-H}) = 15$ Hz, 2, H5_{anti}), 4.60 (m, 2, H2), 1.98 (br s, 2, H1_{outer}), 1.32 (m, 2, H3), 1.00–0.78 (complex overlapping m, 12, phosphine bridging CH_2 's and phosphine ethyl CH_2 's), 0.73–0.52 (br s, 12, phosphine CH_3 's), 0.30 (br s, 2, H1_{inner}). $^{13}\text{C}\{^1\text{H}\}$ NMR (20°C , benzene- d_6): δ 145.9 (s, C4), 106.8 (s, C5), 86.9 (s, C2), 50.8 (s, C3), 29.5 (s, C1), 24.9 (t, phosphine bridging CH_2 's), 14.2 (s, phosphine ethyl CH_2 's), 9.0 (s, phosphine CH_3 's). $^{31}\text{P}\{^1\text{H}\}$ NMR (20°C , benzene- d_6): δ 78.9 (s).

Minor isomer, (syn- η^3 -pentadienyl)(anti- η^3 -pentadienyl)Fe(Et₂PCH₂CH₂PEt₂) (30%). ¹H NMR (20 °C, benzene-*d*₆): δ 6.54 and 6.39 (m, 2, H4's), 5.28 and 5.20 (d, 2, H5's), 5.00–4.95 (d, 2, H5's), 4.71 and 4.07 (m, 2, H2's), 1.87–1.67 (m, 2, H1_{outer} and H3), 1.60–1.35 (m, 2, H1_{outer} and H3), 1.00–0.52 (complex overlapping m, 24, phosphine H's), -0.12 (d of d, $J(\text{H-H}) = 12.5$ Hz, $J(\text{H-P}) = 18$ Hz, 1, H1_{inner}), -0.28 (d of d, $J(\text{H-H}) = 9$ Hz, $J(\text{H-P}) = 9$ Hz, 1, H1_{inner}). ¹³C{¹H} NMR (20 °C, benzene-*d*₆): δ 147.4 and 146.2 (s, C4's), 107.3 and 105.2 (s, C5's), 88.6 and 87.3 (s, C2's), 53.1 and 51.8 (s, C3's), 33.7 and 26.5 (d, C1's), 24.6 and 23.4 (t, phosphine bridging CH₂'s), 15.3 and 15.0 (s, phosphine ethyl CH₂'s), 8.9 and 7.6 (s, phosphine CH₃'s). ³¹P{¹H} NMR (20 °C, benzene-*d*₆): δ 82.5 (d, $J(\text{P-P}) = 36$ Hz), 69.8 (d, $J(\text{P-P}) = 36$ Hz).

(η^3 -Pentadienyl)Fe(Et₂PCH₂CH₂PEt₂)₂⁺BF₄⁻ (2)

HEt₂PCH₂CH₂PEt₂⁺BF₄⁻ (0.294 g, 1.00 × 10⁻³ mol) and (η^3 -pentadienyl)₂Fe(Et₂PCH₂CH₂PEt₂) (1) (0.400 g, 1.01 × 10⁻³ mol) were stirred at room temperature in 75 ml THF for 2 h. The solvent was then removed under reduced pressure leaving a red powder. The powder was washed with two 25 ml portions of diethyl ether and collected on a fine frit. Crystals were obtained by cooling a concentrated solution of **2** in a 10 : 1 THF/toluene mixture to -30 °C. Yield of crude powder: 0.56 g (90%). Anal. Found: C, 48.62; H, 8.55. C₂₅H₅₅FeP₄BF₄ calcd.: C, 48.26; H, 8.91%.

Compound **2** crystallized as (*syn- η^3 -pentadienyl*)Fe(Et₂PCH₂CH₂PEt₂)₂⁺BF₄⁻. However, in solution this species existed in equilibrium with a second isomer, presumably (*anti- η^3 -pentadienyl*)Fe(Et₂PCH₂CH₂PEt₂)₂⁺BF₄⁻. At -40 °C, the two isomers were present in almost equal concentrations.

Isomer mixture. ¹H NMR (-40 °C, acetone-*d*₆): δ 5.94 (broad m, 2, H4's), 5.02 (d, $J(\text{H-H}) = 7.9$ Hz, 1, H5), 4.97 (d, $J(\text{H-H}) = 7.7$ Hz, 1, H5), 4.86 (d, $J(\text{H-H}) = 10.4$ Hz, 1, H5), 4.80 (d, $J(\text{H-H}) = 10.0$ Hz, 1, H5), 4.67 (broad t, 1, H2), 4.25 (broad t, 1, H2), 3.40 (broad s, 1, H1_{outer}), 2.52 (broad q, 1, H3), 2.15–0.70 (overlapping complex m, 96, phosphine H's), 1.80 (broad s, 1, H1_{outer}), 1.49 (broad s, 2, H3 and H1_{inner}), 0.75 (broad s, 1, H1_{inner}). ¹³C{¹H} NMR (-40 °C, acetone-*d*₆): δ 143.7 and 142.7 (s, C4's), 112.7 and 111.4 (s, C5's), 88.7 and 88.2 (s, C2's), 60.4 and 57.0 (s, C3's), 28.5–8.0 (complex overlapping multiplets, C1's and phosphine C's). ³¹P{¹H} NMR (-40 °C, acetone-*d*₆): Complicated 64 line pattern (two overlapping second-order ABCD patterns). Spin simulation yielded the following chemical shifts and coupling constants:

Isomer 1: δ 66.4 (A), 68.6 (B), 75.0 (C), 76.0 (D). $J_{\text{AB}} = 45.1$ Hz, $J_{\text{AC}} = 12.6$ Hz, $J_{\text{AD}} = 45.1$ Hz, $J_{\text{BC}} = 29.4$ Hz, $J_{\text{BD}} = 68.5$ Hz, $J_{\text{CD}} = 57.6$ Hz.

Isomer 2: δ 69.9 (A), 70.6 (B), 76.6 (C), 78.1 (D). $J_{\text{AB}} = 32.6$ Hz, $J_{\text{AC}} = 65.1$ Hz, $J_{\text{AD}} = 7.3$ Hz, $J_{\text{BC}} = 65.1$ Hz, $J_{\text{BD}} = 47.8$ Hz, $J_{\text{CD}} = 47.8$ Hz.

Single crystal X-ray diffraction studies of 1 and 2

Suitable crystals of **1** and **2** were mounted in glass capillaries under inert atmosphere. Data were collected at room temperature using graphite-monochromated Mo-*K*_α radiation. Three standard reflections were measured every 100 events as check reflections for crystal deterioration and/or misalignment. Data reduction and refinement were done using the Enraf-Nonius SDPVAX structure determination package (modified by B.A. Frenz and Assoc., Inc., College Station, TX) on a VAX

Table 5

X-Ray diffraction structure summary

<i>Crystal parameters and data collection summary</i>		
compound:	1	2
formula:	C ₂₀ H ₃₈ FeP ₂	C ₂₅ H ₅₅ FeP ₄ BF ₄
formula weight:	396.32	526.18
crystal system:	orthorhombic	triclinic
space group:	<i>Pbcn</i> (No. 60)	<i>P1</i> (No. 1)
<i>a</i> , Å:	11.347(1)	10.070(2)
<i>b</i> , Å:	9.718(2)	10.756(1)
<i>c</i> , Å:	19.938(3)	8.3622(1)
α , deg:	90.0	112.04(2)
β , deg:	90.0	94.93(1)
γ , deg:	90.0	68.05(1)
<i>V</i> , Å ³ :	2198.6(6)	777.1(3)
<i>Z</i> :	4	1
crystal dimensions, mm:	0.5 × 0.5 × 0.2	0.8 × 0.4 × 0.4
crystal color:	dark red	orange-red
<i>D</i> _{calc} , g/cm ³ :	1.197	1.124
diffractometer model:	Nicolet <i>P3</i>	Nicolet <i>P3</i>
radiation, Å:	Mo- <i>K</i> _α , 0.71069	Mo- <i>K</i> _α , 0.71069
scan type:	θ : 2 θ	Wyckoff
scan rate, deg/min:	variable; 4.0 to 29.3	variable; 3.0 to 29.3
scan range:	1.2 degrees 2 θ below <i>K</i> _{α1} to 1.2 degrees 2 θ above <i>K</i> _{α2}	1.2 degrees ω
2 θ range, degrees:	3.0 to 55.0	4.0 to 55.0
data collected:	<i>h</i> (0 to 14), <i>k</i> (0 to 25), <i>l</i> (0 to 12)	<i>h</i> (0 to 14), <i>k</i> (-12 to 12), <i>l</i> (-11 to 11)
total decay:	negligible	negligible
<i>Treatment of intensity data and refinement summary</i>		
No. of unique data:	2915	2028
No. of data with <i>I</i> > 3 σ (<i>I</i>):	905	1991
Mo- <i>K</i> _α linear abs. coeff., cm ⁻¹ :	8.27	7.13
Abs. correction applied:	ψ -scans	ψ -scans
data-to-parameter ratio:	8.6:1	6.4:1
<i>R</i> ^a :	0.0577	0.0348
<i>R</i> _w ^a :	0.0774	0.0418
GOF ^b :	1.59	0.759
Largest residual peak in diff. Fourier, e/Å ³ :	0.60	0.45

^a $R = \sum ||F_o| - |F_c|| / \sum |F_o|$. $R_w = [\sum w(|F_o| - |F_c|)^2 / \sum w |F_o|^2]^{1/2}$. $w = 1/\sigma^2(|F_o|)$. ^b GOF = $[\sum w(|F_o| - |F_c|)^2 / (N_{obs} - N_{var})]^{1/2}$.

11/780 computer. Crystal data and details of data collection and structure analysis are summarized in Table 5 [10*].

The position of the iron atom in **1** was determined from a Patterson map; it resided on a two-fold rotation axis. The remaining non-hydrogen atoms were found by successive full-matrix least-squares refinements and difference Fourier map calculations. Following anisotropic refinement of the nonhydrogen atoms in **1**, the hydrogen atoms (except for those in the ethylene bridge of the depe ligand) were placed at idealized positions (C-H = 0.95 Å), riding upon their respective carbon

atoms, given fixed isotropic thermal parameters ($B = 8.0 \text{ \AA}^2$), and used in the structure factor calculations but not refined. The C–C single bond in the ethylene bridge of the depe ligand (C12–C12') appears to be anomalously short (1.24(2) Å), but this is probably an artifact of a minor unresolved two-fold disorder in the positions of the bridge carbons [11*]. This explanation is supported by the elongated thermal ellipsoids of carbons C12/C12'.

The structure of **2** was successfully solved in space group $P\bar{1}$ (No. 1), after initial attempts in $P\bar{1}$ (No. 2) failed. Supporting the selection of $P\bar{1}$ were (a) the unit cell volume of $777.1(3) \text{ \AA}^3$, which was consistent with one molecule per unit cell and (b) the lack of inversion center symmetry in the molecule, which ruled out the possibility of the molecule residing on a special position in $P\bar{1}$.

The iron atom in **2** was placed at the origin (0,0,0). Remaining non-hydrogen atoms were found by successive full-matrix least-squares refinements and difference Fourier map calculations. Following anisotropic refinement of the non-hydrogen atoms in **2**, the hydrogen atoms were placed at idealized positions, riding upon their respective carbon atoms, given fixed isotropic thermal parameters ($B = 5.0 \text{ \AA}^2$ for pentadienyl hydrogens, 6.0 \AA^2 for phosphine methylene hydrogens, and 8.0 \AA^2 for phosphine methyl hydrogens), and used in the structure factor calculations, but not refined. The absolute structure of **2** was determined by comparing the R factor of the final structure (0.0348) and its enantiomorph (0.0350). The absolute structure was taken as the structure with the lower R factor.

Summary

Two new electron-rich (pentadienyl)iron(depe) (depe = $\text{Et}_2\text{PCH}_2\text{CH}_2\text{PEt}_2$) complexes have been synthesized and fully characterized. (η^3 -Pentadienyl) $_2\text{Fe}(\text{depe})$ (**1**) is obtained in high yield upon treatment of $(\text{Cl})_2\text{Fe}(\text{depe})_2$ with two equivalents of potassium pentadienide. This species is converted to $(\eta^3\text{-pentadienyl})\text{Fe}(\text{depe})_2^+\text{BF}_4^-$ (**2**) upon treatment with one equivalent of $\text{Hdepe}^+\text{BF}_4^-$. Both **1** and **2** crystallize with their η^3 -pentadienyl ligands bonded in the *syn* geometry. However, in solution, these *syn*- η^3 -pentadienyl complexes exist in equilibrium with isomers possessing *anti*- η^3 -pentadienyl ligands.

Acknowledgment

Support from the National Science Foundation (Grants CHE8520680 and CHE-9003159) is gratefully acknowledged. Washington University's X-Ray Crystallography Facility was funded by the National Science Foundation's Chemical Instrumentation Program (Grant CHE-8811456). The High Resolution NMR Service Facility was funded in part by National Institutes of Health Biomedical Research Support Instrument Grant 1 S10 RR02004 and by a gift from Monsanto Company.

Supplementary material available: Listings of final atomic coordinates, thermal parameters, bond lengths, bond angles, and observed and calculated structure factor amplitudes for **1** (11 pages) and **2** (22 pages) are available from the authors.

References and notes

- 1 Pentadienyl-Metal-Phosphine Chemistry. 21. The previous papers in this series are the following: (a) J.R. Bleeke and J.J. Kotyk, *Organometallics*, 2 (1983) 1263; (b) J.R. Bleeke and M.K. Hays, *ibid.*, 3

- (1984) 506; (c) J.R. Bleeke and W.-J. Peng, *ibid.*, 3 (1984) 1422; (d) J.R. Bleeke and J.J. Kotyk, *ibid.*, 4 (1985) 194; (e) J.R. Bleeke and W.-J. Peng, *ibid.*, 5 (1986) 635; (f) J.R. Bleeke, G.G. Stanley and J.J. Kotyk, *ibid.*, 5 (1986) 1642; (g) J.R. Bleeke and D.A. Moore, *Inorg. Chem.*, 25 (1986) 3522; (h) J.R. Bleeke and A.J. Donaldson, *Organometallics* 5 (1986) 2401; (i) J.R. Bleeke and M.K. Hays, *ibid.*, 6 (1987) 486; (j) J.R. Bleeke, J.J. Kotyk, D.A. Moore and D.J. Rauscher, *J. Am. Chem. Soc.*, 109 (1987) 417; (k) J.R. Bleeke and M.K. Hays, *Organometallics*, 6 (1987) 1367; (l) J.R. Bleeke and W.-J. Peng, *ibid.*, 6 (1987) 1576; (m) J.R. Bleeke, A.J. Donaldson and W.-J. Peng, *ibid.*, 7 (1988) 33; (n) J.R. Bleeke, D.J. Rauscher and D.A. Moore, *ibid.*, 6 (1987) 2614; (o) J.R. Bleeke, M.K. Hays and R.J. Wittenbrink, *ibid.*, 7 (1988) 1417; (p) J.R. Bleeke and A.J. Donaldson, *ibid.*, 7 (1988) 1588; (q) J.R. Bleeke and D.J. Rauscher, *ibid.*, 7 (1988) 2328; (r) J.R. Bleeke and P.L. Earl, *ibid.*, 8 (1989) 2735; (s) J.R. Bleeke and D.J. Rauscher, *J. Am. Chem. Soc.*, 111 (1989) 8972; (t) J.R. Bleeke, R.J. Wittenbrink, T.W. Clayton, Jr., and M.Y. Chiang, *ibid.*, 112 (1990) 6539.
- 2 (a) R.D. Ernst, *Chem. Rev.*, 88 (1988) 1251; (b) R.D. Ernst, *Acc. Chem. Res.*, 18 (1985) 56; (c) H. Yasuda and A. Nakamura, *J. Organomet. Chem.*, 285 (1985) 15. (d) P. Powell, in R. West and F.G.A. Stone (Eds.), *Advances in Organometallic Chemistry*, Vol. 26, Academic Press, New York, 1986, p. 125. (e) S.-F. Lush, S.-H. Wang, G.-H. Lee, S.-M. Peng, S.-L. Wang, R.-S. Liu, *Organometallics*, 9 (1990) 1862 and references therein.
- 3 J. Chatt and R.G. Hayter, *J. Chem. Soc.*, (1961) 5507.
- 4 H. Yasuda, Y. Ohnuma, M. Yamauchi, H. Tani and A. Nakamura, *Bull. Chem. Soc. Jpn.*, 52 (1979) 2036.
- 5 See, for example, Refs. 1b, 1d, 1o, 1q, and 2e. See also: (a) G.-H. Lee, S.-M. Peng, M.-Y. Liao and R.-S. Liu, *J. Organomet. Chem.*, 312 (1986) 113; (b) G.-H. Lee, S.-M. Peng, T.-W. Lee and R.-S. Liu, *Organometallics*, 5 (1986) 2379; (c) G.-H. Lee, S.-M. Peng, F.-C. Liu, D. Mu, and R.-S. Liu, *ibid.* 8 (1989) 402.
- 6 To our knowledge, the only other example of an " $(\eta^3\text{-allyl})\text{FeP}_4^+$ " complex is $(\eta^3\text{-allyl})\text{Fe}\{\text{P}(\text{OMe})_3\}_4^+$: (a) E.L. Muetterties and J.W. Rathke, *J. Chem. Soc., Chem. Commun.*, (1974) 850; (b) S.D. Ittel, F.A. Van-Catledge, and J.P. Jesson, *J. Am. Chem. Soc.*, 101 (1979) 6905.
- 7 C.A. Tolman, *Chem. Rev.*, 77 (1977) 313.
- 8 Similar mechanisms have been postulated for the protonations of $(\eta^3\text{-pentadienyl})_2\text{Fe}(\text{PMe}_3)_2$ [1k] and $(\eta^5\text{-pentadienyl})(\eta^3\text{-pentadienyl})\text{Fe}(\text{PEt}_3)$ [1t].
- 9 A similar solution-phase mixture of isomers is observed for $(\eta^3\text{-pentadienyl})\text{Mn}(\text{Me}_2\text{PCH}_2\text{CH}_2\text{PMe}_2)_2$ [1d].
- 10 Atomic scattering factors were obtained from International Tables for X-Ray Crystallography, Vol. IV, Kynoch Press, Birmingham, England, 1974.
- 11 Disorder of this type is common among $-\text{CH}_2-\text{CH}_2-$ linkages.